

Stopping Cross Sections of Some Hydrocarbon Gases for 40–250 keV Protons and Helium Ions*†

JOHN T. PARK‡ AND E. J. ZIMMERMAN
University of Nebraska, Lincoln, Nebraska

(Received 15 April 1963)

The stopping cross sections of air, He, CH₄, C₂H₂, C₂H₄, C₃H₈, (CH₂)₃, and C₃H₆ have been measured for protons in the energy range 40 to 250 keV. The stopping cross sections of C₂H₄ and C₃H₈ were also measured for helium ions. The data are in good agreement with previous experimental work, and have standard deviations between 1.5 and 4%. They clearly demonstrate the failure of the Bragg rule of additivity for proton energies less than 150 keV. The helium-ion data indicate that the effect of chemical binding on stopping cross sections is unlikely to be any greater for incident helium ions than for incident protons at the same energy.

I. INTRODUCTION

THE loss of energy of slow ions passing through matter has been of interest for a long time, but an adequate theory of stopping power in the low-energy range (less than 400 keV for protons and 2 MeV for helium ions) does not really exist. At higher energies the Bethe theory gives quite accurate predictions of the energy-loss cross sections with the aid of one experimental parameter and the application of the Bragg rule of additivity. In the low-energy range not only is the theory invalid for atomic materials, but the Bragg rule fails. Therefore, it is still necessary to obtain experimental information on each material for which the stopping cross section is needed.

In this experiment the stopping cross sections of air, methane, acetylene, and ethylene were measured as a check on previous work and the stopping cross sections of propane, propylene, and cyclopropane were measured to extend the data available for a study of the failure of the Bragg rule, with particular reference to hydrocarbons.

A differentially pumped gas cell containing a known length of gas at a known temperature and pressure was placed between analyzing and spectrometer magnets. A monoenergetic beam of protons or helium ions was deflected 90° in the field of the magnetic spectrometer when the gas cell was evacuated. The energy change of the exit beam when a gas was admitted to the stopping cell was determined by measuring the decrease in the magnetic field necessary to restore the beam to the original 90° deflection angle. Previous work concerning energy-loss cross-section measurements has been reviewed by Whaling,¹ Allison and Warshaw,² Bethe and Ashkin,³ Taylor,⁴ Uehling,⁵ and Dalgarno.⁶

* Part of a thesis submitted by one of the authors (J.T.P.) to the University of Nebraska in partial fulfillment of the requirements for the degree of Doctor of Philosophy.

† Supported by the U. S. Atomic Energy Commission.

‡ During 1963–1964 at the Physics Department, University College, London, England.

¹ W. Whaling, in *Handbuch der Physik*, edited by S. Flügge (Springer-Verlag, Berlin, 1958), Vol. 34, p. 193.

² S. K. Allison and S. D. Warshaw, *Rev. Mod. Phys.* **25**, 779 (1953).

³ H. Bethe and J. Ashkin, in *Experimental Nuclear Physics*, edited by E. Segrè (John Wiley & Sons, Inc., New York, 1953).

II. APPARATUS

A. Accelerator

The proton and helium-ion beams used in this experiment were produced by the University of Nebraska Cockcroft-Walton accelerator, using a radio-frequency ion source. The accelerator was attached to a carefully calibrated high-voltage resistance divider⁷ from which a small fraction of the accelerating voltage was compared to a preset voltage by a potentiometer. Any difference in voltage was corrected by an electromechanical feedback system⁸ which maintained the accelerating voltage to within 0.01% of the desired voltage.

B. Stopping Cell

The stopping device consists of a differentially pumped gas cell, shown in Fig. 1. The stopping cell is made of a 3-in.-o.d. brass tube 20.307±0.001 cm in length. The ends of this tube are sealed with two disks containing 0.025-in.-diam apertures.

The stopping cell is mounted concentrically inside a 5½-in.-i.d. tube which provides the first differential pumping section. The gas entering this section through the apertures in the gas cell was removed by a 550-liter/sec diffusion pump. This tube extends beyond the

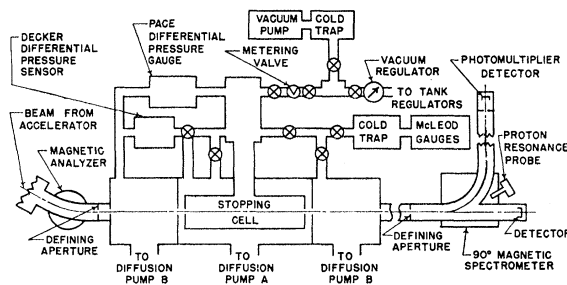


FIG. 1. Diagram of stopping cell and associated equipment.

⁴ A. E. Taylor, *Rept. Progr. Phys.* **15**, 49 (1952).

⁵ E. A. Uehling, *Ann. Rev. Nucl. Sci.* **4**, 325 (1954).

⁶ A. Dalgarno, in *Atomic and Molecular Processes*, edited by D. R. Bates (Academic Press Inc., New York, 1962).

⁷ L. H. Sohl, Master's thesis, University of Nebraska, 1960 (unpublished).

⁸ C. J. Cook and W. A. Barrett, *Rev. Sci. Instr.* **24**, 638 (1953).

ends of the gas cell and is sealed by disks containing 0.050-in.-diam apertures. The sum of the separations between the stopping cell and the ends of the first differential pumping section is 3.589 ± 0.002 cm.

To each end of the $5\frac{1}{4}$ -in. tubing is connected a 4-in.-long piece of 6-in.-o.d. brass tubing terminated by a disk with a 0.100-in.-diam aperture. Gas entering these spaces from the apertures in the first differential pumping section was removed by a second 550-liter/sec diffusion pump.

A 0.025-in.-diam defining aperture is located 50 cm from the end of the stopping cell between the stopping cell and the spectrometer magnet. This aperture narrowed the angle of acceptance to 5 min.

The stopping cell is connected through separate valves to the diffusion pump, the McLeod gauges, the mechanical pressure gauges, and the gas source.

C. Gas-Source Arrangement

The tanks containing the gases to be tested were connected to pressure regulators which were connected through shutoff valves to a vacuum regulator. The low-pressure side of the vacuum regulator was connected by a valve to a stainless steel container which served as a ballast. A valve connected this chamber to a liquid-nitrogen cold trap and a Cenco Hypervac-4 mechanical pump which served to pump the manifold, lines, and regulators free of residual gases. Another valve connected the ballast chamber to a metering valve which was connected to the stopping cell through a high-vacuum shutoff valve.

D. Temperature Measurement

The temperature of the gas was determined by four chromel-alumel thermocouples attached to the stopping cell. The potential was read by either a potentiometer or a potentiometric recorder.

The temperature of the stopping cell was also measured by a mercury thermometer in contact with the $5\frac{1}{4}$ -in. tube surrounding the gas cell. This thermometer was compared over the range being used with a thermometer calibrated by the National Bureau of Standards.

E. Pressure Measurement

The pressure was measured by two mechanical differential pressure gauges which were carefully calibrated by McLeod gauges. The sensitivity of the Pace differential pressure gauge⁹ was increased by placing it in a rectifying bridge. A pressure change of one micron resulted in an output change of 0.04 mV. In normal running conditions a change of 0.01 mV could be detected and the bridge rebalanced.

⁹ Model P1D, 0 to ± 0.1 psi, Pace Engineering Company, North Hollywood, California.

The sensor of the Decker pressure meter¹⁰ has a temperature coefficient of $\pm 0.9\%/^{\circ}\text{C}$. To eliminate this source of uncertainty the sensor was surrounded with spun-glass insulation and then placed inside an insulated metal box, the temperature of which was held constant to $\pm 0.06^{\circ}\text{C}$ by a thermistor temperature control. The output of the Decker pressure meter was connected to a potentiometer. A displacement from pressure equilibrium of 0.1μ resulted in a 2.0-mV output signal. In normal running conditions a change of 0.1 mV could be detected and the potentiometer rebalanced to eliminate it. The drift in zero was negligible, being less than $\pm 0.1 \mu/\text{h}$.

The Decker differential pressure meter proved to be more reliable and more sensitive than the Pace gauge. For these reasons the Pace gauge was used only for the acetylene and methane stopping cross sections and thereafter was used only to check the readings obtained on the Decker differential pressure meter.

The pressure in the first differential pumping section was also measured by the Decker pressure meter. This was done by turning the three-way stopcock connected to one of the ports of the Decker pressure meter. It was found to be unnecessary to measure this pressure for all the readings, as the pressure in this region was a constant fraction of the stopping-cell pressure. The plot of the pressure in the first differential pumping section against inner chamber pressure is a straight line independent of the gas to the smallest pressure the Decker meter can accurately measure.

The pressure of the outer differential pumping sections as measured by an ion gauge remained below 5×10^{-5} mm Hg.

Two McLeod gauges were used as the ultimate pressure reference. One was constructed and calibrated in an earlier experiment,¹¹ and the other McLeod gauge was calibrated by the manufacturer.¹² The two gauges agreed within 0.6%, and the average reading was used.

F. Magnetic Spectrometer

The energy loss of the beam in passing through the gas sample was determined with the aid of a 90° magnetic spectrometer. The current in the magnet coils could be held constant to 0.01% for periods of 15 min or more. The magnetic field was measured with a proton resonance magnetometer based on the transitron circuit of Knoebel and Hahn.¹³

When the resonance signal was obtained, the frequency of the oscillator was measured with a General Radio type 620A frequency meter, reading directly between 10 and 20 Mc/sec with harmonics extending the range from 5 to 40 Mc/sec. The frequency meter

¹⁰ Model 306-2F, 0- to ± 0.3 -in. H_2O , The Decker Corporation, Bala-Cynwyd, Pennsylvania.

¹¹ C. S. Cook, E. Jones, and T. Jorgensen, Phys. Rev. **91**, 1417 (1953).

¹² Model GM100A, Consolidated Vacuum Company, Rochester, New York.

¹³ H. Knoebel and E. Hahn, Rev. Sci. Instr. **22**, 904 (1951).

could be calibrated against a crystal oscillator at no less than three places on each range of the scale. It was generally possible to determine the resonance frequency to better than ± 0.002 Mc/sec.

G. Detector

The beam of protons or helium ions was detected by an electron multiplier (DuMont 6292) from which the glass tube had been removed. The beam of ions passed through a set of narrow slits and struck the first dynode of the electron multiplier. The amplified current was taken from the last dynode. A Keithley Model 610 electrometer was used to read the current.

III. METHOD

With the stopping cell and differential pumping gap evacuated, the analyzing magnet was adjusted so that the beam of protons or helium ions from the accelerator entered the stopping cell. After passing through the stopping cell the beam entered the magnetic spectrometer which was adjusted to deflect the beam into the 90° detector. Gas was then admitted to the stopping cell and the spectrometer magnet readjusted to deflect the beam leaving the stopping cell into the 90° detector. The energy dependence of the beam current leaving the stopping cell is shown in Fig. 2 for the stopping cell evacuated and with gas admitted to the stopping cell. In each case the spectrometer magnet was adjusted for maximum beam current.

The pressures of the gas in the stopping cell were generally in the pressure range 0.05- to 0.5-mm Hg. Pressures as high as 1.8-mm Hg were used with acetylene and methane, and up to 3.0-mm Hg for helium. The gas pressure used was a function of the gas being used and the energy of the incident beam. Gas pressures which were too high resulted in excessive attenuation of the beam and an energy distribution of the exit beam too broad to permit accurate location of the maximum. At the extremely low pressures the energy losses were too small in relation to the energy distribution of the incident beam and resulted in large errors in the energy-loss measurements.

The energy loss, ΔE , is determined from the fact that when the beam is deflected 90° into the detector, $E = kf^2$, where f is the frequency of the nuclear resonance and k is a constant determined by the geometry of the deflecting magnet, the properties of the nuclear resonance magnetometer, and the incident ion. The measured value of k was 0.985 ± 0.002 keV/Mc² for protons and 0.256 ± 0.001 keV/Mc² for helium ions with individual measurements lying within $\frac{1}{2}\%$ of these values. Defining E_1 as the energy and f_1 as the resonance frequency corresponding to the incident beam and E_2 and f_2 the corresponding quantities for the beam after having passed through the gas, we find

$$\Delta E = k(f_1^2 - f_2^2) = E_1 \left(\frac{f_1 - f_2}{f_1} \right) \left[2 - \left(\frac{f_1 - f_2}{f_1} \right) \right].$$

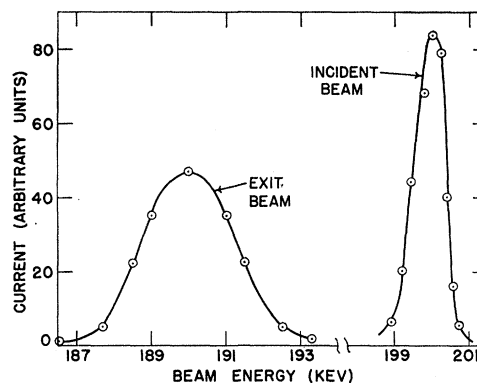


FIG. 2. Energy distributions of an incident and exit 200-keV proton beam incident on helium (2.749 mm Hg).

The stopping power of a gas in terms of the energy loss cross section per molecule is $\epsilon = (1/N)(\Delta E/\Delta x)$, where ϵ will be given in 10^{-15} eV-cm² per molecule. Δx is given by the accumulation of effective path length. The number of molecules per cubic centimeter, N , is obtained by reducing the gas to standard conditions, using the ideal-gas law and the definition of Loschmidt's number, A :

$$N = A \left(\frac{273}{T + 273} \right) \left(\frac{P}{760} \right),$$

where T is the temperature in degrees Centigrade, and P is the pressure in mm Hg. Combining these results gives the working equation

$$\epsilon = \frac{1}{A} \left(\frac{T + 273}{273} \right) \left(\frac{760}{P} \right) \left(\frac{f_1 - f_2}{f_1} \right) \times \left[2 - \left(\frac{f_1 - f_2}{f_1} \right) \right] \left(\frac{E_1}{L + L'P'/P} \right),$$

where L is the length of the stopping cell. L' is the length, and P' is the pressure of the first differential pumping section.

The data obtained in the experiment were reduced by a Burroughs-205 computer which calculated both the stopping cross sections and the uncertainty in them for each experimental measurement. The points which were used to determine the cross-section curves were the weighted averages of five to nine experimental measurements.

IV. ERROR ANALYSIS

A. Energy

The energy of the proton beam from the accelerator has been found to be directly proportional to the reading on the calibrating potentiometer at the energies where the nuclear resonances of F^{19} , B^{11} , and Mg^{24} occur.⁷ The uncertainty in the energy at resonance was less than

TABLE I. Uncertainty in stopping cross sections due to impurities.

Gas	Minimum purity	Uncertainty due to impurities (%)
Acetylene	99.5 ^a	0.2
Cyclopropane	99.5 ^a	0.2
Ethylene	99.5 ^a	0.2
Methane	99.0 ^a	0.5
Propane	99.5 ^a	0.3
Propylene	99.0 ^a	0.3
Helium	99.995 ^b	0.1

^a Matheson Company, Incorporated.^b Amarillo, Texas, Helium Plant (U. S. Bureau of Mines).

0.5%. This fact, plus the linearity of the graph of beam energy against resonance frequency of the magnetometer, indicates that the energy over the entire energy range is within 0.5% of the voltage setting. The energy enters twice into the reduction of the experimental data in such a way that the maximum error in the stopping cross section due to the uncertainty in energy is 0.7%.

B. Energy Loss

Examination of the energy distribution shows that both incident beam and exit beam are very symmetrical, especially near their maxima. (See Fig. 2.) The width of the incident beam at half-maximum depended slightly upon the focusing of the accelerator but was approximately $\frac{1}{2}$ % of the beam energy. The peak of the incident beam could be located to better than ± 0.1 % of the incident-beam energy. The energy spread of the beam depended on the gas in the stopping cell, the energy loss, and the energy of the incident beam. The uncertainty in the energy of the exit beam was about 10% of the energy spread at half maximum. The energy loss sustained by the beam varied between 2 and 15 keV and the uncertainty resulting from the energy loss varied from 2 to 15% and was necessarily calculated separately for each experimental measurement.

TABLE II. Typical errors in single measurements of the stopping cross sections of propane for 100-keV protons.

Random errors	(%)
Uncertainty in energy loss	3.0
Uncertainty in pressure	1.9
Uncertainty in temperature	0.3
Uncertainty in relative frequency change	1.1
Root-mean-square value	3.7
Systematic errors	(%)
Uncertainty in energy	0.7
Uncertainty in McLeod gauge calibration	0.35
Uncertainty in length	0.01
Uncertainty due to impurities	0.3
Root-mean-square value	0.8

C. Uncertainty due to Impurities

All the hydrocarbon gases were purchased from the Matheson Company, Incorporated. The helium was obtained from the Amarillo, Texas, Helium Plant of the U. S. Bureau of Mines. The air was drawn through a drier using activated alumina. The purity of each gas and the uncertainty resulting from the impurities is given in Table I.

All the gases, except air, are assumed to contain only the impurities specified by the manufacturer. Considerable effort was applied to prevent any contamination of the test gases. The connecting tubing, regulators, and valves were always leak tested and evacuated prior to the opening of the high pressure valve on the tank. The system was flushed with the test gas at least four times prior to the beginning of the stopping-cross-section measurements.

In the case of ethylene, most of the impurities have

TABLE III. Proton stopping cross sections per atom (10^{-16} eV-cm²) of $\frac{1}{2}$ air and helium.

Energy (keV)	Helium (%)		$\frac{1}{2}$ Air (%)	
40	6.72	± 2.6	15.7	± 3.1
50	6.93	± 2.2	16.5	± 2.7
60	7.07	± 1.9	17.00	± 2.1
70	7.15	± 1.7	17.15	± 1.8
80	7.15	± 1.6	17.21	± 1.6
90	7.13	± 1.5	17.20	± 1.4
100	7.05	± 1.4	17.10	± 1.4
110	6.94	± 1.5	16.9	± 1.6
120	6.80	± 1.5	16.65	± 1.6
130	6.65	± 1.5	16.35	± 1.6
140	6.49	± 1.5	16.0	± 1.6
150	6.35	± 1.5	15.7	± 1.6
175	6.02	± 1.6	14.7	± 1.6
200	5.64	± 1.6	13.7	± 1.7
225	5.27	± 1.6	12.9	± 1.7
250	4.87	± 1.8	12.0	± 1.8

larger stopping cross sections than ethylene; hence, the result is to make the experimental cross section of ethylene about 0.2% too high. For this reason, the reported values of the stopping cross section in Table III have been reduced by 0.2% from the measured values.

D. Uncertainty due to Resonance Frequency Measurement

The uncertainty due to the measurement of the resonance frequency of the magnetometer was calculated assuming very conservatively that the frequency could be determined to ± 0.005 Mc/sec. The effect of this uncertainty varied greatly and was calculated for each measurement.

E. Temperature

The temperature was readily determined to within 1°C. Both the mercury thermometer and the thermo-

TABLE IV. Proton stopping cross sections per molecule (10^{-16} eV-cm²) of hydrocarbon gases.

Energy (keV)	Acetylene (%)	Ethylene (%)	Methane (%)	Cyclopropane (%)	Propylene (%)	Propane (%)
40	45.6±3.7	52.0±2.8	38.0±3.3	70.2±3.0	75.7±2.9	83.7±2.9
50	46.7±3.0	55.0±2.7	39.2±3.0	74.5±2.7	79.7±2.6	89.2±2.6
60	47.3±2.8	56.2±2.6	39.8±2.8	76.9±2.3	82.4±2.3	91.8±2.2
70	47.6±2.6	56.7±2.2	40.0±2.3	78.1±2.1	83.0±2.0	92.4±1.7
80	46.9±2.4	56.3±1.6	39.7±2.3	78.0±1.8	82.3±1.8	91.5±1.8
90	45.9±2.2	55.3±1.6	39.1±2.0	77.5±1.8	80.8±1.7	90.2±1.7
100	44.7±2.2	54.1±1.6	38.1±2.0	76.5±1.7	79.5±1.7	88.7±1.7
125	41.7±2.2	51.0±1.6	34.5±2.0	73.3±1.7	75.1±1.6	84.1±1.6
150	38.8±2.2	47.1±1.6	31.4±2.2	69.1±1.6	70.6±1.6	78.7±1.6
175	35.7±2.3	43.8±1.6	29.7±2.6	64.6±1.6	65.8±1.6	73.6±1.6
200	33.1±2.3	41.0±1.6	27.8±2.0	60.6±1.6	61.5±1.6	68.4±1.6
225	31.0±2.5	38.1±1.7	25.9±2.0	56.4±1.6	57.1±1.6	64.4±1.6
250	29.2±2.6	35.4±1.8	23.8±2.0	52.2±1.6	52.6±1.6	59.8±1.6

couples could be read to greater accuracy than this, but due to variations in room temperature there were differences between the readings of the various thermocouples and the mercury thermometer. This difference was usually much less than a degree.

F. Pressure

The uncertainty in the pressure as determined by the Decker meter is less than 2% above 0.05-mm Hg. Below this pressure, the uncertainty is $\pm 1 \mu$. This uncertainty was obtained from the average deviations of the readings when compared to the McLeod-gauge readings in air, the uncertainty in corrections to the Decker-meter calibration, and the uncertainty in the McLeod-gauge readings.

The uncertainty of the pressure measurements made by the Pace gauge is somewhat larger. The Pace gauge was used for measurements on methane and acetylene, and for these gases the pressure uncertainty is estimated as 3.5%.

The uncertainty in the pressure of the gases for which the McLeod gauges were used directly is taken as 0.5%. In addition, the uncertainty in the measurement of the height of the mercury column of the McLeod gauges was taken to be ± 0.005 cm.

G. Uncertainty in the Stopping Cell Length

The uncertainty due to the measurement of the length of the stopping cell and the first differential pumping gap is less than 0.01%. The lengths were corrected for thermal expansion.

H. Propagation of Error

As an example of the errors in a single measurement, Table II shows those for 100-keV protons on propane with an energy loss of 8 keV. These uncertainties have been combined by standard root-mean-square error propagation methods.

Examination of the statistical spread of measure-

ments taken at about the same energy shows the value obtained for the uncertainty by the root-mean-square method to be quite conservative. The statistical spread in the measurements was consistent with a standard deviation for the experimental measurements of about 2% for all the gases except acetylene which had a slightly greater statistical spread.

Five or more measurements at approximately the same energy were weighted and averaged to produce the points which were used to form the curves. The contribution of the random errors to the uncertainty of the final stopping-cross-section curves is further reduced by the process of drawing a smooth curve through the points obtained from the weighted averages of the measurements.

V. RESULTS AND CONCLUSIONS

A. Values of Stopping Cross Sections

The stopping cross sections and their uncertainties are given in Tables III, IV, and V. The values in the tables are taken from smooth curves and the uncertainties shown are the standard deviations of the curves at that point. As the uncertainty in the stopping cross section is a function of energy, energy loss, and the stopping gas, the standard deviations were calculated for each point on the curve from the expected uncertainties and the number of readings taken in the energy interval.

TABLE V. Helium-ion stopping cross sections per molecule (10^{-16} eV-cm²) of ethylene and propane.

Energy (keV)	Ethylene (%)	Propane (%)
40	41.6	± 4.5
70	61.5	± 2.5
100	75.0	± 2.2
130	84.9	± 1.8
160	93.0	± 1.6
200	102.8	± 1.7
250	112.8	± 1.7

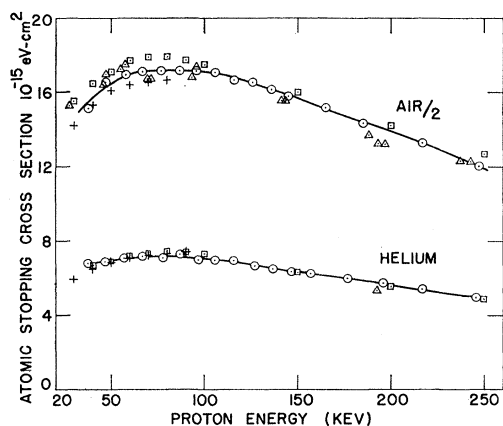


FIG. 3. Proton stopping cross sections of $\frac{1}{2}$ air and helium. \circ Present data, \triangle Weyl (Ref. 14) (data), $+$ Phillips (Ref. 15) (from smooth curves, air = $0.8 \text{ N}_2 + 0.2 \text{ O}_2$), \square Reynolds *et al.* (Ref. 16) (from smooth curves).

B. Comparison with Theory and other Experiments

The present experiment is in very good agreement with prior experiments. (See Fig. 3.) Weyl¹⁴ measured the energy loss in air in the energy range 30 to 450 keV. Excellent agreement is obtained over the entire energy range of the present experiment. Phillips¹⁵ measured the stopping cross sections of oxygen and nitrogen for 10- to 80-keV protons. The cross sections computed for $0.8\text{N}_2 + 0.2\text{O}_2 = \text{air}$ are about 3% lower than the present experiment in the energy range where they can be compared. It must be noted that Phillips measured oxygen and nitrogen and not air. Reynolds *et al.*¹⁶ measured the stopping cross section for 40- to 600-keV protons incident on air. The experimental results obtained by Reynolds *et al.* are about 3% higher than results obtained in the present experiment.

The experimental stopping cross sections obtained by the same experiments for protons incident on helium can also be compared with the present experiment. (See Fig. 3.) The stopping-cross-section curves obtained by Phillips¹⁵ and Reynolds *et al.*¹⁶ are in very good agreement with the present data. The data of Reynolds *et al.* average about 1% higher than the present data. Weyl¹⁴ made one experimental determination of the stopping cross section of helium for protons which is 7% lower than the present stopping-cross-section curve.

The stopping cross section of acetylene, ethylene, and methane were also measured by Reynolds *et al.*¹⁶ The stopping-cross-section curve of Reynolds *et al.* is 1.6% higher for acetylene, 2.5% higher for ethylene, and 3% higher for methane than our data. This dis-

crepancy is not unreasonable for the stated uncertainty of the curves.

As can be seen from Fig. 3, the present data on air and helium appear to lie in the middle of the measurements of other experimenters. In the stopping cross sections of acetylene, ethylene, and methane where only Reynolds *et al.* and the present experiment can be compared, the small discrepancy between the two sets of stopping cross sections is of the size and direction that would be expected from comparisons of the two experiments on air and helium stopping cross sections.

The comparison of range experiments to energy-loss experiments is a somewhat questionable procedure since the extremely narrow angle of acceptance in the energy-loss experiments largely eliminates the fraction of the beam undergoing energy loss due to nuclear scattering. The energy loss determined from range measurements is necessarily larger as a result. Ranges obtained from energy-loss measurements are in question due to the problem of determining energy losses at the end of the range as well as due to the effects of nuclear scattering. If the problem of determining the end of the range is avoided by using the range obtained by Cook, Jones, and Jorgensen¹¹ at 40 keV and integrating the present experimental results from 40 keV to energies less than 250 keV, the ranges obtained agree to better than 3% for methane and 5% for air with the ranges measured by Cook *et al.* Differentiating the range of Cook *et al.* gives energy-loss cross sections for air and methane which, although higher, are within 7% of the present experimental results.

For protons of energy between 40 and 250 keV there is very little theoretical work with which the experiments can be compared. The average excitation energy has been calculated directly for helium by Dalgarno and Lynn.^{6,17} The stopping cross sections for protons incident on helium using this value of the average excitation energy, give satisfactory agreement with the present experimental results to as low as 150 keV. Gryzinski's¹⁸ classical theory of stopping cross sections gives good agreement for protons incident on helium over this entire energy range.

For most of the gases, the Bethe theory is valid only at energies higher than 250 keV. It may be noted, however, that the experimental curves may be extended to fit smoothly onto the theoretical curves. For example, the calculation of the stopping cross section of propane by Brandt¹⁹ can be extrapolated to energies below those at which it is strictly valid to meet the present experimental curve, giving a smooth curve which covers the entire range.

Very few stopping-cross-section data are available for helium ions, and there are no data with which our

¹⁷ A. Dalgarno and N. Lynn, Proc. Phys. Soc. (London) **A70**, 802 (1957).

¹⁸ M. Gryzinski, Phys. Rev. **115**, 374 (1958).

¹⁹ W. Brandt, Research Report, Radiation Physics Laboratory, DuPont de Nemours & Company, Wilmington, Delaware, 1960 (unpublished).

¹⁴ P. K. Weyl, Phys. Rev. **91**, 742 (1953).

¹⁵ J. A. Phillips, Phys. Rev. **90**, 532 (1953).

¹⁶ H. K. Reynolds, D. N. F. Dunbar, W. A. Wenzel, and W. Whaling, Phys. Rev. **92**, 742 (1953).

stopping cross section of helium ions in ethylene or propane can be compared. However, there is no reason to expect any factor, which would affect the calibration of the apparatus, to be a function of the incident ion. For this reason, the helium-ion data are probably as reliable as the proton data. The stopping-cross-section curves of ethylene and propane have the same general shape as those observed by Lorentz and Zimmerman²⁰ for solid hydrocarbons.

Lindhard and Scharff²¹ have calculated the loss of energy to electrons for ion velocities small compared to $\nu_0 Z_1^{3/2}$, where Z_1 is the nuclear charge of the incident ion and ν_0 is the electron velocity in the first Bohr orbit. Their relationship is valid for helium ions with energy less than 250 keV or protons with less than 25 keV. Rewriting their equation in terms of E , the energy of the incident ion, we obtain

$$\epsilon \propto (E/E_0)^{1/2},$$

where E_0 is the kinetic energy of the incident ion when its velocity equals $\nu_0 Z_1^{3/2}$.

In the helium-ion energy range 50–250 keV the energy loss of helium ions is predominately due to the electrons, as can be seen by examining Bohr's²² expression for the nuclear contributions; hence, the above relation can be compared with the experiment in respect to the energy dependence. The experimental results showed some deviation from a direct power dependence on the energy at the lowest energies, and it must be noted that the power dependence on energy can be varied quite strongly without greatly increasing the uncertainty in the fitting of the data. The least-squares fitting to the experimental data for incident helium ions gave $\epsilon = 8.4 E^{0.47}$ for ethylene and $\epsilon = 9.7 E^{0.47}$ for propane. Lorentz and Zimmerman²⁰ data for solid hydrocarbons gave $\epsilon = 5.0 E^{0.44}$ for polyethylene and $\epsilon = 34 E^{0.44}$ for polystyrene. The energy dependence is in general agreement with that obtained by Van Wyngaarden and Duckworth²³ for carbon and aluminum oxide films. The data for ethylene and propane are in somewhat better agreement with Lindhard and Scharff than Van Wyngaarden's data are.

Lorentz and Zimmerman²⁰ found that the ratio (which varied with energy) of the stopping cross section for 100-keV helium ions to that of 100-keV protons was 1.54 ± 0.02 for polyethylene, polystyrene, and Pholite S-5A. The same ratio is 1.38 ± 0.05 in the present experiment. As this is a ratio, systematic errors would tend to cancel for either the solid film or the gas experiments. Only systematic differences which arise as a result of changing the ions would affect this ratio.

²⁰ D. C. Lorentz and E. J. Zimmerman, Phys. Rev. **113**, 1199 (1959).

²¹ J. Lindhard and M. Scharff, Phys. Rev. **124**, 128 (1961).

²² N. Bohr, Kgl. Danske Videnskab. Selskab, Mat. Fys. Medd. **18**, No. 8 (1948).

²³ A. Wyngaarden and H. Duckworth, Can. J. Phys. **40**, 1749 (1962).

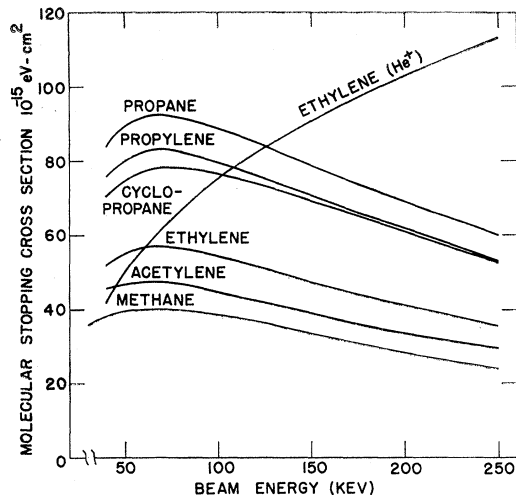


FIG. 4. Proton-stopping cross sections for hydrocarbon gases.

Considering the methods used in the two experiments, such errors are very unlikely since only the gas in the ion source of the accelerator needs to be replaced in order to change from helium ions to protons. Therefore, it is likely that this difference is real and it may reflect a difference in behavior between solids and gases. The fact that the ratio of helium ion to proton data at a given energy is the same for both ethylene and propane, but differs from the value obtained for the three solids, strongly suggests that this difference depends upon the physical state of the substance. There are not sufficient data at present to permit a definite statement as to the cause of these differences in ratios of the stopping powers for helium ions and protons. The lack of such data provides considerable interest for future experiments to examine the effects of physical state and chemical binding on helium-ion stopping cross sections.

C. The Bragg Rule of Additivity

The Bragg rule of additivity for a hydrocarbon molecule can be stated in the form $s(C_m H_n) = ms(C) + ns(H)$, where $s(C_m H_n)$ is the stopping cross section of the hydrocarbon molecule, $C_m H_n$, and $s(C)$ and $s(H)$ are the stopping cross sections of atomic carbon and hydrogen, respectively. The quantity of experimental information that is required to provide desired energy-loss cross sections could be greatly reduced if molecular stopping cross sections could be obtained from atomic stopping cross sections. However, Reynolds *et al.*,¹⁶ Platzman,²⁴ and others have noted that the Bragg rule of additivity fails for protons incident on hydrocarbons in this energy region.

In addition to the usual tests for the validity of the Bragg rule of additivity, the present experiment in-

²⁴ R. L. Platzman, in *Symposium on Radiobiology*, edited by J. J. Nickson (John Wiley & Sons, Inc., New York, 1952).

cludes a very straightforward and simple test for its validity. The failure of the rule is made obvious by Fig. 4 which shows the stopping cross sections of cyclopropane (CH_2)₃ and propylene (C_3H_6). These substances have exactly the same number of carbon and hydrogen atoms but different molecular structure. At higher proton energies the cross sections of the two gases converge; however, at proton energies of less than 100 keV the discrepancy between the propylene and cyclopropane curves is definitely outside the experimental errors. Great care was used to eliminate systematic errors in the stopping cross sections of these two substances so that small differences between the cross sections would be meaningful. For this reason, it is felt that the present experiment clearly illustrates the failure of the Bragg rule of additivity for hydrocarbon gases in the proton energy range below 150 keV and shows the necessity for examining the molecular binding to explain the deviations from the Bragg rule of additivity.

With only the present data it can be stated that the differences due to chemical binding are unlikely to be as large for incident helium ions as for incident protons. In the energy range 150 to 250 keV the helium-ion stopping cross sections for polyethylene reported by

Lorentz and Zimmerman²⁰ are nearly identical with the helium-ion cross section for ethylene obtained in the present experiment. Further, if the Bragg rule values of the atomic stopping cross sections for hydrogen and carbon obtained from the Lorentz and Zimmerman data on solid plastics are used to calculate the stopping cross section of propane for helium ions, the calculated cross section is within 2 to 4% of the experimentally obtained values. Because of the paucity of data on helium ions, the conclusion is somewhat tentative, but it would appear that the stopping of helium ions is less dependent on molecular binding than is the stopping of protons.

ACKNOWLEDGMENTS

We wish to express our gratitude to Dr. Theodore Jorgensen, director of the Nebraska Range-Energy Project for helpful suggestions and assistance, and also to the other members of the project. The cooperation of Chester A. Sautter with whom much of the equipment was shared is especially appreciated. The authors are also indebted to the National Science Foundation for a fellowship for one of us (J.T.P.) and to the Atomic Energy Commission for its continued support of the Nebraska Range-Energy Project.